Available online at www.sciencedirect.com
SCIENCE DIRECT®
Journal of Organometallic Chemistry 674 (2003) 32–37
Journal of Organometallic Chemistry
www.elsevier.com/locate/jorganchem

Ferrocene-histidine conjugates: *N*-ferrocenoyl-histidyl(im*N*-ferrocenoyl)methylester: synthesis and structure

Himadri S. Mandal, Heinz-Bernhard Kraatz *

Department of Chemistry, University of Saskatchewan, 110 Science Place, Saskatoon, Sask., Canada S7N 5C9

Received 25 February 2003; received in revised form 18 March 2003; accepted 19 March 2003

Abstract

The preparation of the new ferrocenoyl histidyl conjugates *N*-Fc-His-OMe (**2**) and *N*-Fc-His(ε-*N*-Fc)-OMe (**3**) and of a simple ferrocenoyl imidazole conjugate Fc-Im (**4**) is reported together with their spectroscopic and electrochemical characterization. The electrochemistry of **3** exhibits two fully reversible one-electron oxidations, which are due to the stepwise oxidation of the two ferrocenoyl groups. The crystal structure of **3** shows the difference in the chemical environment of the two Fc groups, one being attached to the α-N and one being attached to the ε-N of the imidazole of histidine. There is no discernible intermolecular interaction present in the crystal structure.

Keywords: Ferrocene; Histidine; Bioconjugate; Amino acid; X-ray; Electrochemistry

1. Introduction

The design of novel biomaterials has generated significant interest in the synthesis and properties of redox active systems having the redox active organometallic ferrocene function attached to a biological molecule. Potential application of such bioconjugates include biomolecular sensing and switching devices [1]. The ferrocene group can be readily incorporated into a biomolecule, such as a peptide or DNA [2]. In case of ferrocene-labeled peptides, the individual bioconjugates often assemble to give supramolecular systems that show various degrees of inter- and intramolecular hydrogen bonding [3.4]. For example, 1,1′-disubstituted ferrocene-peptide derivatives can act as templates to generate highly ordered electroactive chiral helicates, in which intramolecular but interchain H-bonding between the podand chiral peptide substituents on the two Cp rings of the ferrocene group is responsible for the formation of the supramolecular assembly [3]. In other cases, intermolecular H-bonding gives rise to helical three-dimensional superstructures [4]. Importantly, ferrocene-peptide bioconjugates are able to respond to the structural changes that will take place upon substrate binding to the peptide portion of the molecule [5]. Up to this point this research has mainly focused on interactions involving Fe-peptides with other peptides or neutral molecules.

In metallo-proteins, the imidazole group of histidine is often found as a ligand coordinating to metal ions such as Zn^{2+}, Fe^{2+}, Cu^{2+} and others [6]. Until now, there has been no report of ferrocene-histidine conjugates, which may offer the potential for the development of metal specific probes. In this paper, we give a full account of the preparation and characterization of the first histidine-ferrocene conjugates.

2. Results and discussion

Compounds **2** and **3** are obtained by the reaction of the active ester Fc-OBt (**1**) with H-His-OMe·HCl in dichloromethane in the presence of triethylamine as shown in Scheme 1. The reaction results in the formation of two major products. Compound **2** represents the expected *N*-Fc-His-OMe conjugate, having the Fc group attached to the α-amino group, whereas com-

* Corresponding author. Fax: +1-306-966-4660.
E-mail address: kraatz@sask.usask.ca (H.-B. Kraatz).

0022-328X/03/$ - see front matter © 2003 Elsevier Science B.V. All rights reserved.
doi:10.1016/S0022-328X(03)00182-7

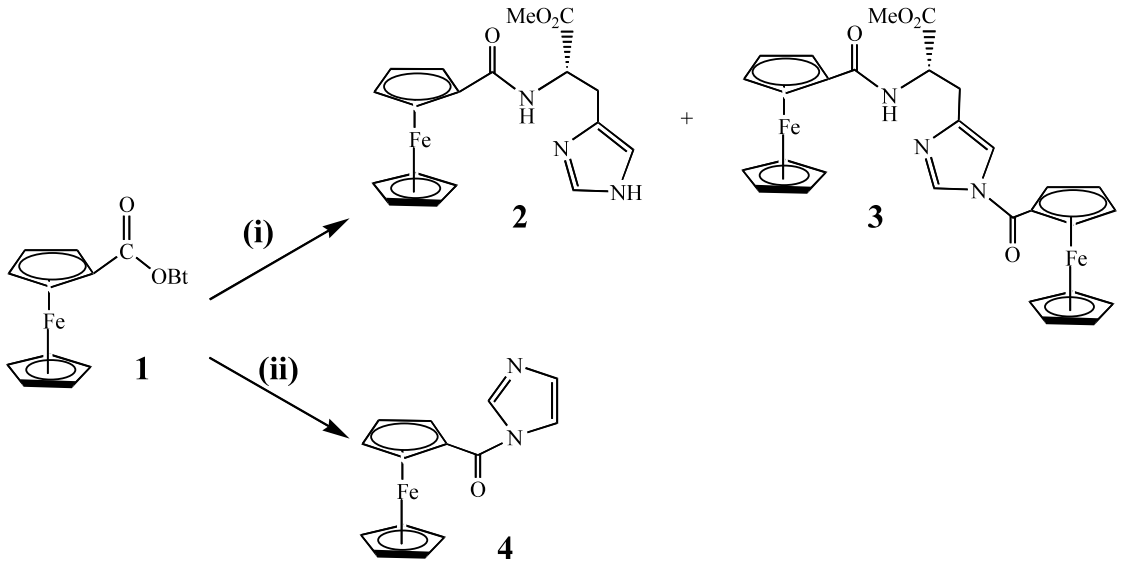

Scheme 1. Synthesis of *N*-Fc-His-OMe (**2**), *N*-Fc-His(ε-*N*-Fc)-OMe (**3**), and Fc-Im (**4**): (i) H-His-OMe·2HCl, CH_2Cl_2, Et_3N; (ii) imidazole, CH_2Cl_2, Et_3N.

pound **3** has an additional Fc label at the ε-N of the imidazole group.

The ^{1}H-NMR spectra of compounds **2** and **3** allow a clear identification. The spectrum of compound **2** shows the presence of a single Fc group, with signals at δ 4.75 for the two ortho-H of the substituted Cp ring of the Fc group, a signal at δ 4.34 for the two meta-H, and a singlet at δ 4.21 for the 5H of the unsubstituted Cp ring. In contrast, the ^{1}H-NMR spectrum of compound **3** shows the presence of two Fc groups. The α-H of compound **2** is observed at δ 4.88, whereas that of compound **3** is slightly shifted downfield to δ 4.97. Similarly, the ^{13}C-NMR shows the presence of an additional third signal in the carbonyl region for compound **3** (δ 172.4, 170.8, 169.0), while for compound **2** only two signals are observed (δ 172.6 and 171.6).

A comparision of the IR spectra of compounds **2** and **3** with that of ferrocenoyl imidazole (**4**) allows the unequivocal assignment of the carbonyl bands. Compound **4** exhibits a single Amide I band at 1695 cm^{-1}. For compound **2**, two bands are observed at 1708 and at 1642 cm^{-1} for the methylester and amide stretch, respectively. Both bands compare well with those observed for other Fc-amino acids and peptides [5]. As expected, compounds **3** exhibit an additional band at 1692 cm^{-1} assigned to the amide of the additional Fc group attached to the ε-N of the histidine imidazole. Interestingly, for **3** the band assigned to the ester stretch is significantly shifted as compared to **2** and is observed at 1739 cm^{-1}. Clearly binding of the additional Fc group to the ε-N of the histidine imidazole has an influence on the Fc group attached to the α-N of His. The UV–vis spectrum of **2** shows a single absorption at $\lambda_{max} = 435$ nm, whereas for **3** the Fc absorption is red-shifted with a λ_{max} of 460 nm, which is identical to the maximum of Fc-imidazole **4**. In order to evaluate if the two Fc groups in compound **3** are electronically coupled, we investigated the solution electrochemistry of compounds **2**–**4** in acetonitrile solution by cyclic voltammetry (CV). Fig. 1 shows the cyclic voltammograms of the di-Fc compound **3** and the mono-Fc compounds **2** and **4** recorded under identical conditions. All compounds exhibit fully reversible redox properties as judged from the separation of cathodic and anodic wave and the ratio of the peak currents. The results are summarized in Table 1. Compound **3** exhibits two fully reversible one-electron oxidation waves at 638(2) and at

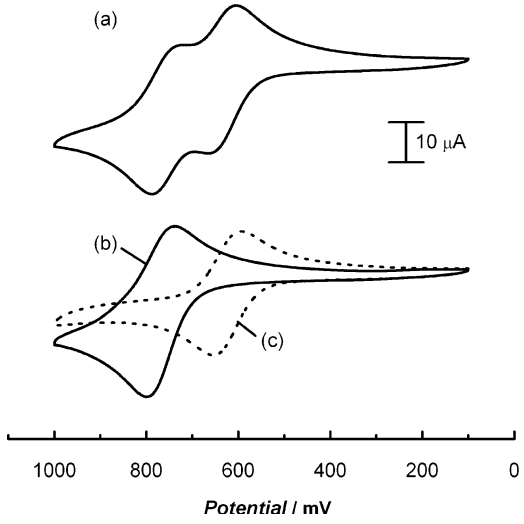

Fig. 1. Cyclic voltammograms of compounds **2**–**4** recorded at 100 m Vs^{-1} in acetonitrile containing 0.1 M TBAP as supporting electrolyte. The concentration of compounds **2**–**4** was 1 mM. The potential is reported vs. the potential of a Ag/AgCl reference electrode. *N*-Fc-His-OMe (**2**): (c), *N*-Fc-His(ε-*N*-Fc)-OMe (**3**): (a), Fc-Im (**4**) (b).

Table 1
Electrochemical properties of *N*-Fc-His-OMe (**2**), *N*-Fc-His(ε-*N*-Fc)-OMe (**3**), and Fc-Im (**4**) at 100 mV s^{-1} in acetonitrile containing 0.1 M TBAP as supporting electrolyte at 20(2) °C

Compound	$E_{1/2}$ (mV)	ΔE (mV)	i_{pa}/i_{pc}
N-Fc-His-OMe (**2**)	630(2)	65(3)	1.04
N-Fc-His(ε-*N*-Fc)-OMe (**3**)	638(2)	60(2)	1.11
	762(4)	61(5)	1.04
Fc-Im (**4**)	768(1)	66(2)	1.11

A Glassy carbon electrode was employed as the working electrode, together with a platinum counter electrode and a Ag/AgCl reference electrode.

762(4) mV (vs. Ag/AgCl). A comparison with compounds **2** and **4** allows the assignment of the two waves to the individual redox groups. The redox event at a half-wave potential of 638(2) mV is assigned to the Fc group attached to the a-N of His and the second wave at $E_{1/2} = 762(3)$ mV is assigned to the Fc attached to the e-N of the imidazole group. By comparison compound **2** gives a single wave at $E_{1/2} = 630(2)$ mV and compound **4** exhibits a wave at $E_{1/2} = 768(1)$ mV. Importantly, the two redox events observed in compound **3** are only slightly shifted from the position of the mono-Fc systems, indicating that possible coupling between the two redox centers is only small.

In order to confirm the structure of compound **3** as having two Fc groups, one attached to the a-N and one to the e-N of the imidazole of the His group, we crystallized compound **3** from CH_2Cl_2 solution giving orange prismatic crystals, allowing its structural investigation by X-ray crystallography. A structural representation of compound **3** is shown in Fig. 2 and clearly shows the presence of two Fc groups in the molecule — one at the α-amino terminus and one at the ε-N of imidazole group. The orientation of the two Fc group is such that two H atoms of the Fc(2) point to the face of the unsubstituted Cp ring of Fc(1). The distance between the H of Fc(2) and the face of the Cp ring of Fc(1) are about 3.5 Å. Such interaction have been observed before in aromatic systems [7]. The packing diagram shows the absence of strong intermolecular H-bonding interactions involving the amide N–H, which are often found for Fc-amino acids and peptides in solution and the solid state. The Cp–CO lengths in **3** are significantly different between the two chemically and electrochemically different Fc groups. The Fc-group attached to the α-N of His exhibits a Fc–CO distance of 1.489(3) Å, whereas the second Fc group, which is attached to the ε-N of the imidazole group, shows a significantly shorter Fc–CO bond distance of 1.475(4) Å, potentially reflecting a greater electronic interaction of the Cp and imidazole group. However, both bond distances are well within the parameters for Fc-amides [8]. The amide group of Fc(2) shows a significant twist with regards to the Fc group of 28.1° and of 9.5° with regards to the imidazole group. The angle between the Cp, the amide, and the imidazole does not prevent electronic coupling between the amide, the Cp, and the imidazole. It is interesting to note that the Cp and imidazole groups are not co-planar (twist of 36.5°). The two Cp rings of Fc(2) are co-planar (bent of 2.6°), as are the two Cp rings of Fc(1) (bent of 2.1°).

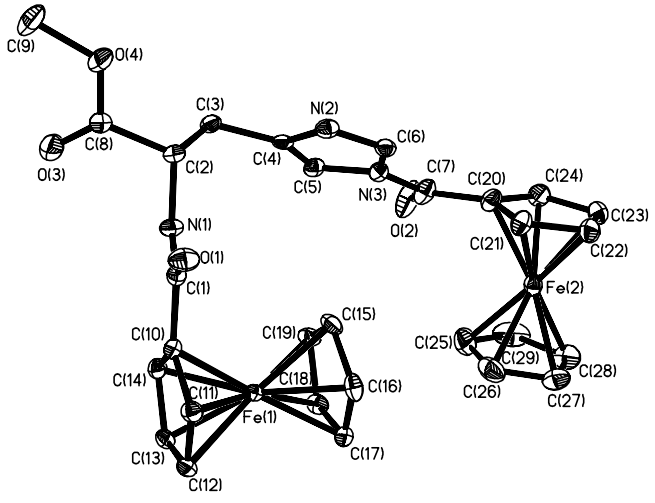

Fig. 2. ORTEP drawing of *N*-Fc-His(ε-*N*-Fc)-OMe (**3**) shown with 30% probability ellipsoids. All hydrogen atoms are omitted for clarity. Selected bond distances and angles: O(1)–C(1) = 1.226(3) Å, O(2)–C(7) = 1.204(3) Å, N(1)-C(1) = 1.343(3) Å, N(1)–C(2) = 1.446(3) Å, N(3)–C(7) = 1.412(3) Å, C(1)–C(10) = 1.489(3) Å, C(3)–C(4) = 1.506(3) Å, C(4)–C(5) = 1.343(3) Å, C(7)–C(20) = 1.475(4) Å, N(1)–C(1)–C(10) = 114.9(2)°, N(3)–C(7)–C(20) = 118.8(2)°, N(3)–C(7)–C(20) = 118.8(2)°.

However, the Cp/amide twist is less pronounced for Fc(1) attached to the α-N of histidine (11.8°). In general, amide/Cp twists for Fc-amino acids and peptides are about 5–20°. However, in some cases strong intermolecular interactions may be responsible for slightly larger twists.

3. Conclusions

We have investigated the reactivity of Fc-OBt (**1**) with H-His-OMe allowing the isolation of two previously unknown ferrocenoyl histidine conjugates of *N*-Fc-His-OMe (**2**) and *N*-Fc-His(ε-*N*-Fc)-OMe (**3**). The electrochemistry of compound **3** shows a large difference between the two redox potentials of the two Fc groups. The Fc group attached to the ε-N of the imidazole is much more difficult to oxidize giving a $E_{1/2}$ of 762(4) mV (vs. Ag/AgCl). This represents only a small shift compared to $E_{1/2}$ of Fc-Im at 768(1) mV, indicating that, if at all, only a small interaction appears to exist between the two Fc electrophores. The crystal structure of **3** confirms the proposed structure with Fc(1) being attached to the α-N of His and Fc(2) being attached

to the ε-N of the imidazole group of His. Compound **2** is of future interest since it has an available coordination site available for metal coordination. Although only a small interaction appears to exist in the di-Fc compound **3**, we are hopeful that coordination of metal centers to the imidazole ring in compound **2** will result in changes of the redox potential of the Fc reporter of **2**. We will report about these investigations in due course.

4. Experimental

4.1. General

Ferrocenoylbenzotriazole ester (FcOBt) was prepared as described earlier [2g]. H-His-OMe·2HCl (Aldrich) was used as received. CH_2Cl_2 was dried over CaH_2 and distilled under nitrogen prior to use. Et_3N (Aldrich) was used without any further purification. ^1H were recorded at 300.135 and 75.478 MHz, respectively on a Bruker AMX 300 NMR spectrometer. ^{13}C spectra were recorded on a Bruker FBR 500 MHz spectrometer at 125.797 MHz. All chemical shifts (δ) are reported in ppm and coupling constants (J) in Hz. $CDCl_3$ (Aldrich) used for NMR spectroscopy was stored over molecular sieves (8–12 mesh; 4 Å effective pore size; Fisher). ^1H-NMR shift are referenced to the non-deutero impurity in $CDCl_3$ (δ 7.24) and are reported relative to tetramethylsilane (δ 0.00). Assignments in the ^1H and $^{13}C\{^1H\}$-NMR were made using J-modulation and ^1H–^1H COSY experiments. All measurements were carried out at 293 K unless otherwise specified. Mass spectrometry was carried out on a VG analytical 70/20 VSE instrument.

4.2. Reaction of FcOBt with H-His-OMe·2HCl

Et_3N (3 ml) was added to a suspension of H-His-OMe·2HCl (0.26 g, 1.05 mmol) in CH_2Cl_2 (10 ml). After 10 min the mixture was added to a solution of FcOBt (0.35 g, 1 mmol) in CH_2Cl_2 (25 ml) and was stirred for 16 h at room temperature. The mixture was then extracted with aqueous solutions of 10% citric acid, saturated $NaHCO_3$ and distilled water, respectively. The remaining organic phase was dried over anhydrous $MgSO_4$, filtered and evaporated in *vacuo* leaving a reddish solid which, purification by flash column chromatography containing a solvent mixture of acetone/hexane (2:3) yielded two products *N*-Fc-His-OMe ($R_f = 0.04$, 13%) (**2**) *N*-Fc-His(ε-*N*-Fc)-OMe (**3**) ($R_f = 0.43$, 23%) as the major products.

4.3. Characterization of N-Fc-His-OMe (2)

UV–vis (λ_{max} in nm, ε in $mol^{-1}\,l\,cm^{-1}$): 437 (135). IR (KBr, cm^{-1}): 1708 (C=O, ester), 1642 (C=O, amide). ^1H-NMR ($CDCl_3$, δ): 7.77 (1H, d, $J_{HH} = 5.5$ Hz, NH Im), 7.64 (1H, s, H_a Im), 6.94 (1H, s, H_c Im), 4.88 (1H, m, H^{α}), 4.75 (2H, m, Ho Cp), 4.34 (2H, d, $J_{HH} = 1.5$ Hz, H_m Cp), 4.21 (5H, s, H_u Cp), 3.71 (3H, s, His-CH_3), 3.16 (2H, m, C^{β}). ^{13}C-NMR ($CDCl_3$, δ): 172.6 (C=O His-CO_2Me), 171.6 (C=O NHCO Fc-His), 135.7 (C_1 Im), 135.5 (C_3 Im), 115.7 (C_2 Im), 75.6 (C_i Cp), 71.0 (C_m Cp), 70.2 (C_u Cp), 68.9 (C_o Cp), 68.7 (C_o Cp), 53.2 (CH_3 His), 52.7 (C^{α} His), 29.3 (C^{β} His). HRMS (FAB, glycerol+PEG) *m/z* Calc. for $C_{18}H_{19}N_3O_3Fe$ $[M+1]^+$: 382.0854, found: 382.0859.

4.4. Characterization of N-Fc-His(ε-N-Fc)-OMe (3)

UV–vis (λ_{max} in nm, ε in $mol^{-1}\,l\,cm^{-1}$): 460 (640). IR (KBr, cm^{-1}): 1739 (C=O, ester), 1692 (C=O, amide, imidazole), 1640 (C=O, amide).^1H-NMR ($CDCl_3$, δ): 8.35 (1H, s, H_a Im), 7.50 (1H, s, H_b Im), 7.47 (1H, s, NH NHCO), 4.97 (1H, m, Hα), 4.92 (2H, br. s, H_o Cp Fc-Im), 4.76 (2H, dd, $J_{HH} = 14$, 1.6 Hz, H_o Cp Fc-His), 4.64 (2H, t, $J_{HH} = 1.9$ Hz, H_m Cp Fc-Im), 4.35 (2H, t, $J_{HH} = 1.8$ Hz, H_m Cp Fc-His), 4.26 (5H, s, H_u Cp Fc-Im), 4.24 (5H, s, H_u Cp Fc-His), 3.76 (3H, s, His-CH_3), 3.18 (2H, m, H^{β}). ^{13}C-NMR ($CDCl_3$, δ): 172.4 (C=O His-CO_2Me), 170.8 (C=O of Fc at ε-N Im), 169.0 (C=O NHCO Fc-His), 139.4 (C_1 Im), 137.4 (C_3 Im), 115.6 (C_2 Im), 72.4 (C_i Cp Fc His), 72.0 (C_i Cp Fc-His), 71.0 (C_u Cp Fc-Im), 70.2 (C_i Cp Fc-His), 69.0 (C_m Cp Fc-Im), 68.5 (C_m Cp Fc-His), 59.0 (Cα NHCO), 52.8 (C_o Cp Fc-Im), 52.4 (C_o Cp Fc-His), 24.2 (CH_3), 20.0 (C^{β}). HRMS (FAB, NBA+PEGH) *m/z* Calc. for $C_{29}H_{27}N_3O_4Fe_2$ $[M+1]^+$: 594.0779, found: 594.0769.

4.5. Synthesis of Fc-Im (4)

Et_3N (1 ml) was added to a solution of imidazole (0.082 g, 1.2 mmol) in CH_2Cl_2 (5 ml) and the mixture was then added to a solution of FcOBt (0.347 mg, 1 mmol) in CH_2Cl_2 (25 ml). After stirring for 16 h at room temperature. The reaction mixture was extracted, dried and evaporated as described above to give a reddish solid. Purification by flash column chromatography containing a solvent mixture of acetone/CH_2Cl_2 (1:5) gave the desired product Fc-Im (**4**) ($R_f = 0.44$, 66%). IR (KBr, cm^{-1}): 1695 (C=O, amide imidazole). UV–vis (λ_{max} in nm, ε in $mol^{-1}\,l\,cm^{-1}$): 460 (805). ^1H-NMR ($CDCl_3$): 8.40 (1H, s, H_a Im), 7.67 (1H, s, H_c Im), 7.13 (1H, s, H_b Im), 4.93 (2H, t, $J_{HH} = 2.1$ Hz, H_o Cp), 4.65 (2H, t, $J_{HH} = 2.1$ Hz, H_m Cp), 4.28 (5H, s, H_u Cp).

4.6. Electrochemical studies

All electrochemical experiments were carried out using a CV-50W Voltammetric Analyzer (BAS) at room temperature (20(2) °C). No special precautions were taken to exclude oxygen. All CV were recorded in

Table 2
Crystal data and structure refinement for *N*-Fc-His(ε-*N*-Fc)-OMe (**3**)

Empirical formula	$C_{29}H_{27}Fe_2N_3O_4$
Formula weight	593.24
Temperature (K)	193(2)
Wavelength (Å)	0.71073
Crystal system	Orthorhombic
Space group	$P2_12_12_1$
Unit cell dimensions	
a (Å)	5.7934(5)
b (Å)	18.6857(15)
c (Å)	23.4160(18)
V (Å^3)	2534.9(4)
Z	4
D_{calc} (g m^{-3})	1.554
Absorption coefficient (mm^{-1})	1.187
$F(0\,0\,0)$	1224
Crystal size (mm)	$0.55 \times 0.19 \times 0.12$
θ range for data collection (°)	1.74–26.38
Limiting indices	$-7 < h < 7$, $-23 < k < 23$, $-28 < l < 29$
Reflections collected	14667
Independent reflections	5182
Data/restraints/parameters	5182/0/343
GooF (F^2)	1.077
Final R indices [$I > 2\sigma(I)$]	$R = 0.0300$, $wR = 0.0680$
R indices (all data)	$R = 0.0337$, $wR = 0.0694$
Abs. structure parameter	0.000(13)
Largest diff. peak and hole (eÅ^{-3})	0.48 and −0.21

freshly distilled acetonitrile (dired over CaH_2). Tetrabutylammonium perchlorate (TBAP) was used as supporting electrolyte (0.1 M). For the CV studies a glassy carbon working electrode (BAS, diameter 2 mm) and a platinum wire counter electrode were used. The glassy carbon working electrode was polished with 3 μm followed by 1 μm, then 0.5 μm alumina prior to use to remove any surface contaminants, which was followed by ultrasonication in distilled water to remove excess alumina. The reference electrode was a Ag/AgCl electrode (BAS). iR compensation was applied to all experiments. Solvent backgrounds were collected before each set of experiments and then subtracted from the spectra. The analyte concentration in all cases was 1 mM. Experiments were repeated at least 5 times with freshly prepared solutions of the analyte.

4.7. X-ray crystallography

Orange crystals of **3** were obtained by layering a solution of **3** in CH_2Cl_2 with n-hexane. A prismatic crystal was mounted on a glass fiber using epoxy resin. The data set was collected on a Siemens SMART CCD diffractometer MoKα radiation (graphite monochromated). The structure of **3** was solved by direct methods using the SHELXTL [9]. All non-hydrogen atoms were refined anisotropically using full-matrix least squares to give the final R values of $R = 0.0300$ and $wR = 0.0680$ for 5182 observed reflections ($I > 2\sigma(I)$). All crystallographic details have been summarized in Table 2.

5. Supplemental material

Crystallographic data excluding structure factors have been deposited at the Cambridge Crystallographic Data Centre (CCDC 203143). This material can be obtained upon request to CCDC, 12 Union Road, Cambridge, CB2 1EZ, UK (http://www.ccdc.cam.ac.uk; email: deposit@ccdc.cam.ac.uk).

Acknowledgements

The authors wish to thank NSERC for financial support. H-B. K. is the Canadian Research Chair in Biomaterials. We thank Bob McDonald, X-ray Crystallography Laboratory, Department of Chemistry, University of Alberta, for collecting the data set for compound **3**.

References

[1] (a) J.D. Schmitt, M.S.P. Sansom, I.D. Kerr, G.G. Lunt, R. Eisenthal, Biochemistry 36 (1997) 1115;
(b) E.C. Constable, Angew. Chem. Int. Ed. Engl. 30 (1991) 407.
[2] (a) A. Anne, A. Bouchardon, J. Moiroux, J Am Chem. Soc. 125 (2003) 1112;
(b) C.J. Yu, Y. Wan, H. Yowanto, J. Li, C. Tao, M.D. James, C.L. Tan, G.F. Blackburn, T.J. Meade, J. Am. Chem. Soc. 123 (2001) 11155;
(c) A. Anne, B. Blanc, J. Moiroux, Bioconjugate Chem. 12 (2001) 396;
(d) C.J. Yu, H. Wang, Y. Wan, H. Yowanto, J.C. Kim, L.H. Donilon, C. Tao, M. Strong, Y. Chong, J. Org. Chem. 66 (2001) 2937;
(e) T. Ihara, M. Nakayama, M. Murata, K. Nakano, M. Maeda, Chem. Commun. (1997) 1609;
(f) T. Ihara, Y. Maruo, S. Takenaka, M. Takagi, Nucleic Acids Res. 24 (1996) 4273;
(g) H.-B. Kraatz, J. Lusztyk, G.E. Enright, Inorg. Chem. 36 (1997) 2400;
(h) P. Saweczko, G.D. Enright, H.-B. Kraatz, Inorg. Chem. 40 (2001) 4409;
(i) A. Hess, J. Sehnert, T. Weyhermuller, N. Metzler-Nolte, Inorg. Chem. 39 (2000) 5437;
(j) C.-Z. Li, Y.-T. Long, H.-B. Kraatz, J.S. Lee, J. Phys. Chem. B. 107 (2003) 2291.
[3] (a) A. Nomoto, T. Moriuchi, S. Yamazaki, A. Ogawa, T. Hirao, Chem. Commun. (1998) 1963;
(b) T. Moriuchi, A. Nomoto, K. Yoshida, A. Ogawa, T. Hirao, J. Am. Chem. Soc. 123 (2001) 68;
(c) T. Moriuchi, A. Nomoto, K. Yoshida, A. Ogawa, T. Hirao, Organometallics 20 (2001) 1008;
(d) T. Moriuchi, K. Yoshida, T. Hirao, J. Organomet. Chem. 637–639 (2001) 75.

[4] I. Bediako-Amoa, R. Silerova, H.B. Kraatz, Chem. Commun. (2002) 2430.
[5] P. Saweczko, G.D. Enright, H.-B. Kraatz, Inorg. Chem. 40 (2001) 4409.
[6] A. Messerschmidt, R. Huber, T. Poulos, K. Wieghardt (Eds.), Handbook of Metalloproteins, Wiley, Toronto, 2001.
[7] G.R. Desiraju, T. Steiner, The Weak Hydrogen Bond, Oxford University Press, Oxford, 1999.
[8] L. Lin, A. Berces, H.-B. Kraatz, J. Organomet. Chem. 556 (1998) 11.
[9] (a) G.M. Sheldrick, Acta Crystallogr. A46 (1990) 467;
(b) G.M. Sheldrick, SHELXS-97, University of Göttingen, Germany, 1990;
(c) G.M. Sheldrick, SHELXL-93, University of Göttingen, Germany, 1993.